

# Evaluation of Pre-processing in Road Pavement Image Analysis

Henrique Oliveira<sup>†‡</sup>, Paulo Lobato Correia<sup>†</sup>

<sup>†</sup> Instituto de Telecomunicações, Instituto Superior Técnico, Av. Rovisco Pais 1, 1049-001 Lisboa, Portugal

Phone: +351-218418455, Fax: +351-218418472, e-mail: [hjmo@lx.it.pt](mailto:hjmo@lx.it.pt), [plc@lx.it.pt](mailto:plc@lx.it.pt)

<sup>‡</sup> ESTIG – Instituto Politécnico de Beja, Rua Afonso III, 1, 7800-050 Beja, Portugal, Phone +351-234377900, Fax 234378157

**Abstract** — This paper addresses the problem of automatic detection and classification of road pavement surface cracks by the analysis of images acquired during road pavement surface surveys. In particular, pre-processing techniques and their combination are discussed and evaluated. Local statistics, as the mean and standard deviation of pixel intensities, computed for non-overlapping image regions, are considered. The various pre-processing techniques are combined in different orders, to evaluate their impact in adequately modelling the feature space and thus leading to the best distress detection results. A set of well-know metrics is used for the evaluation, to conclude about the best pre-processing order.

## I. INTRODUCTION

Cracks are the most common road pavement surface defects, requiring an adequate rehabilitation management policy. The search for an automated surface defect detection system is an active research topic, aiming to reduce the subjectivity of human operators during the traditional visual inspection methodologies and contributing to develop a safer and less labor intensive procedure.

Digital images are typically the most important source of information for qualitative and quantitative crack distress evaluation. Neural networks, Markov random fields, edge detectors and morphological operators have been considered for the development of automatic crack distress detection systems [1] [2].

This paper considers a new approach for road pavement surface defects analysis, combining image processing and pattern recognition techniques. Here, the processing of non-overlapping image regions based on local statistics (mean and standard deviation of block pixel intensities) is used for the pre-processing of images before feature space construction. Features are then processed by a pattern classifier, labeling image regions as either containing crack pixels or not. This pattern classifier is supervised, consisting of training and test stages.

This paper is organized as follows: in section II the proposed pre-processing strategies, as well as the crack detection classifier, are described. Section III presents experimental results and section IV draws some conclusions and presents some hints for future work.

## II. IMPLEMENTATION DETAILS

The proposed road pavement surface crack detection system

processes images at a region level instead of pixel based. Images are divided into non-overlapping regions of  $75 \times 75$  pixels, as this was empirically found to provide a good ratio between computational complexity and accuracy.

For each region, two features are computed: the mean and the standard deviation of the gray level values. In the present work, an image database containing 56 gray level images with size  $2048 \times 1536$  pixels, acquired by a digital camera with its optical axis perpendicular to the pavement surface, are considered. The database is split into two distinct sets: Training Set Images (TIS) and Testing Set Images (TTIS), using the methodology proposed in [3]. Two sample images containing cracks are shown in Figure 1, the left one being used for training, while the right image belongs to the test set.

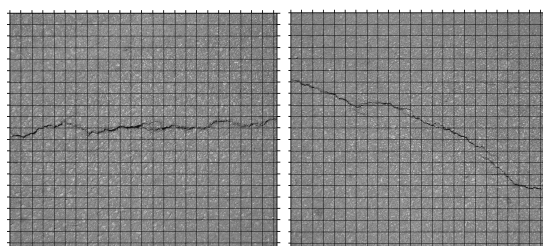


Fig. 1. Sample database images (training image on the left and testing image on the right side figure), showing the subdivision into distinct blocks.

The system architecture of the proposed supervised crack detection and classification system is represented in Figure 2.

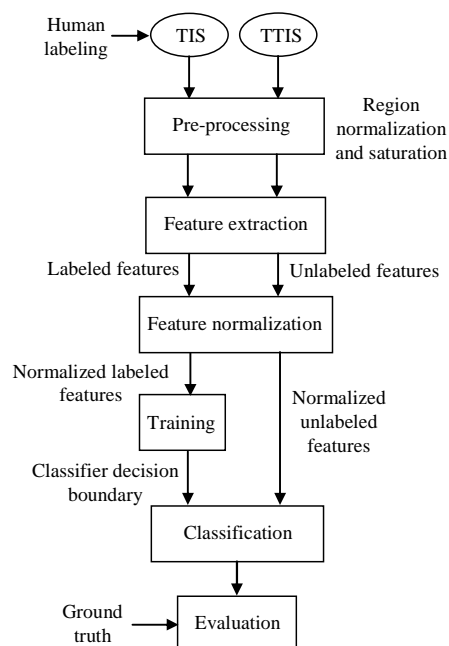


Fig. 2. Proposed system architecture.

In the following, the two main components of the pre-processing module, intensity normalization and saturation, are described and their combination is discussed.

### A. Region intensity normalization

To improve the classification results, it is important to ensure that the input data is adequately normalized, so that image acquisition imperfections and the variability inherent to this type of images, such as variations in road surface materials reflectance, have a minimal impact in the classification results [2].

One step in this direction, is computing a reference gray level value ( $rglv$ ) for all regions in each image, taken as the mean value of all gray levels in the available regions. Image normalization is performed at the region level, ensuring that all regions in each image present the same mean gray level value.

For each image a matrix with the average pixel intensity values within regions is computed (mean matrix), with its dimensions,  $nl_{mm}$  and  $nc_{mm}$ , given by:

$$nl_{bm} = \text{fix}\left(\frac{nl_{img}}{75}\right) \text{ and } nc_{bm} = \text{fix}\left(\frac{nc_{img}}{75}\right), \quad (1)$$

where  $nl_{img}$  and  $nc_{img}$  stand for the number of image lines and columns, respectively, and  $\text{fix}$  is an operator rounding a number towards zero.

As image regions containing cracks tend to present average pixel intensities lower than those not having crack pixels, their normalization procedure is performed differently. This requires a preliminary identification of regions with cracks according to the methodology described in [3]. Each mean matrix is scanned, vertically and horizontally, to find local minima in each column or line of the mean matrix. Regions likely to contain cracks should present average pixel intensities lower than a given threshold, computed taking into account the mean of average intensity values of vertical or horizontal neighbors and also the mean and the standard deviation of all average intensity values, along the scan direction (entire column or row), see equations (2) and (4) respectively in [3]. At this stage, a binary matrix is created where regions likely to contain crack pixels are labeled '1'. Figure 3 shows a region normalization example, ensuring that all regions without cracks present the same mean gray level (right side of figure) in opposition to the original image (left side of figure).

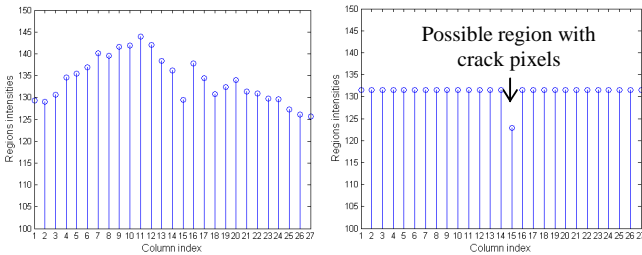


Fig. 3. Region average intensity levels along one row of the mean matrix computed over the original (left) and normalized (right) images.

Both graphs in Figure 3 reveal that the relevant lower average pixel intensities for regions likely to contain crack pixels are maintained.

### B. Region intensity saturation

Another important component of the pre-processing module exploits specific knowledge about the characteristics of cracks, which are expected to correspond to darker image areas. As such, any pixel within a block with a value above the computed  $rglv$  for each image can be set to the value of  $rglv$ , as illustrated in Figure 4. This allows simplifying the input images, reducing noise and thus the global variance of gray level values in non crack regions, without losing any relevant crack information.

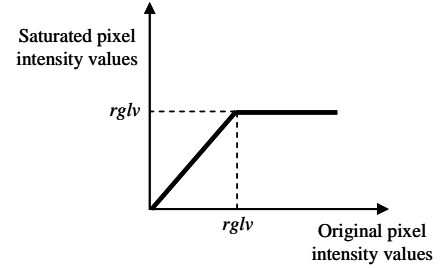


Fig. 4. Region intensity saturation function.

The effects of applying the saturation function to reduce the variance of non crack input regions is illustrated in Figure 5, by displaying the values of standard deviation of pixel intensities within regions ( $std$  matrix). The two graphs show how the  $std$  values along an image row is better suited to identify crack regions after applying the saturation function. In fact, higher amplitude differences between the  $std$  values of the two object classes are observed after intensity saturation.

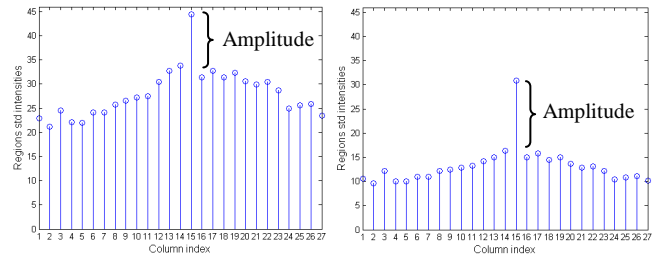


Fig. 5. Regions intensity standard deviation values for a row in the  $std$  matrix, computed for original (left) and saturated (right) images.

### C. Combining normalization and saturation techniques

The procedures described in the previous sections may be applied over the entire image database in different orders. The normalization of region intensities can be followed by region intensity saturation, or vice-versa. In order to better show the effects of these two procedures, scatter plots are constructed for both cases, with the horizontal axis representing region average intensities, while the vertical axis corresponds to the standard deviation values.

Figure 6 shows the case where intensity normalization is followed by the intensity saturation, and Figure 7 represents

the case where the opposite processing order is considered. Comparing the two scatter plots, it can be noted that, in Figure 6, the points representing the *no cracks region* class seem to be adequately modeled by normal distributions, while in Figure 7 they tend to be aligned along straight lines. The points labeled by the human operator as *regions with crack pixels* seem to have a more disperse distribution in both cases, when compared to the *regions without crack pixels* class.

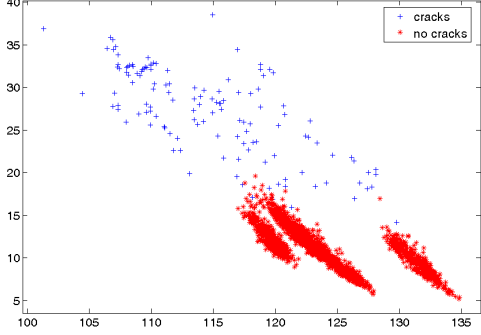


Fig. 6. Scatter plot representing regions for TIS images (five images), considering intensity normalization followed by intensity saturation operations.

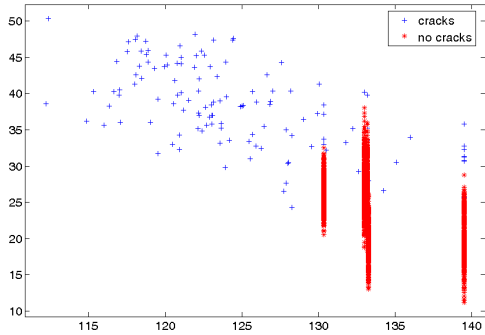


Fig. 7. Scatter plot representing regions for TIS images (five images), considering intensity saturation followed by intensity normalization operations.

#### D. Feature extraction and normalization

For the proposed system, a two dimensional feature space is constructed based on two simple features: the mean and standard deviation of pixels intensities within each non-overlapping image region. Once features are available, another normalization step is carried out, to reduce the feature representation scattering among database images, which would negatively influence the classification results. For each database image, the centroid of its two dimensional feature space is calculated (median values of coordinates along horizontal and vertical axis). Then, a global centroid is computed (mean value of all image centroid coordinates), and, for each individual image, the two dimensional feature space points are translated so that the respective centroid coincides with the global centroid. An example of feature space representation after this normalization step, applied over the same data used to create Figures 6 and 7, is shown in Figures 8 and 9, respectively, where the horizontal axis represents the average region intensity values and the vertical axis corresponds to standard deviation values.

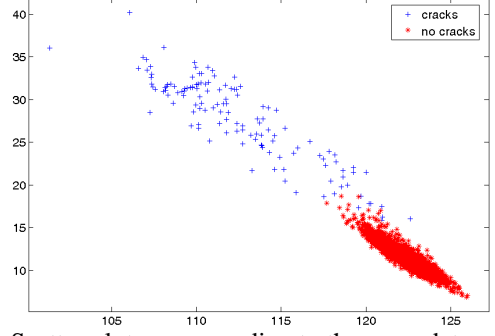


Fig. 8. Scatter plot corresponding to the same data used for Figure 6, after applying the feature space normalization.

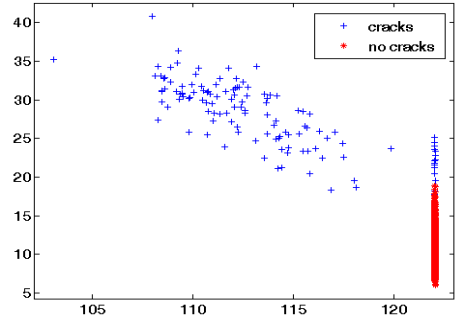


Fig. 9. Scatter plot corresponding to the same data used for Figure 7, after applying the feature space normalization.

#### E. Crack region detection

To classify each region as containing crack pixels or not, the available measurements (mean and standard deviation of gray levels values within a region) for each image are used to compose a pattern vector  $\mathbf{x}$ , representing a sample of the random variable  $\mathbf{X}$ , taking values on a sample space  $\mathcal{X}$ . For each element  $x_i$  of the pattern vector  $\mathbf{x}$  one possible class  $y_i$  is assigned, where  $\mathcal{Y}$  is the class set. Thus, the training set is:

$$T = \{(x_1, y_1) \dots (x_n, y_n) : x_i \in \mathcal{X}^2; y_i \in \{c_1, c_2\}\}, \quad (2)$$

where  $n$  is the number of points for the pattern vector  $\mathbf{x}$ .  $y_i$  is assumed to be a hidden variable. Only two classes are used: *regions with crack pixels* ( $c_1$ ) and *regions without crack pixels* ( $c_2$ ).

A classification of unlabeled image regions into the considered classes can be made according with Bayes theorem, using a uniform cost function. The decision rule [4] is symbolically represented by:

$$p(\mathbf{x} | y_i = c_1)P(y_i = c_1) \underset{c_2}{\overset{c_1}{>}} p(\mathbf{x} | y_i = c_2)P(y_i = c_2) \quad (3)$$

where the class priors  $p(y_i = c_k)$  for  $k \in \{1, 2\}$ , are calculated according with:

$$p(y_i = c_k) = \frac{\# \text{ measurements labeled into class } c_k}{\text{total number of measurements for all classes}}, \quad (4)$$

Since a general covariance matrix was adopted, the boundary decision is quadratic. The decision boundaries

obtained with the TIS using the two different combinations of the pre-processing modules are shown in Figure 10, for the feature spaces presented in Figures 8 and 9.

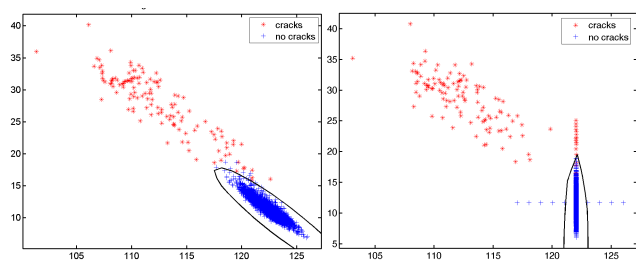


Fig. 10. Boundary decisions computed using the feature spaces show in Figure 8 (left) and Figure 9 (right). In the second case, 10 points (five on each side of *region without crack pixels* class) were added for computational stability.

### III. PERFORMANCE EVALUATION

The performance of the implemented pre-processing strategies has been evaluated on a set of real pavement surface images, acquired along a Portuguese road. Part of the algorithmic development was supported by the PRtools toolbox [5].

Intraclass and interclass distances [6] are shown in Table I for the distribution of region values observed in the considered TIS (five images from the entire image database).

Table I  
Intraclass and interclass distances.

Procedures	Intraclass (crack regions)	Intraclass (no crack regions)	Interclass
Norm + Saturation	87.18	8.65	402.44
Saturation + Norm	90.21	7.95	366.52
Original	147.90	145.00	395.80

Classes' separability could be evaluated by the intraclass to interclass ratio. According to the values listed in Table I, the first pre-processing approach presents the best *no crack* regions intraclass to interclass distances ratio (0.0215 against 0.0217 obtained by the second processing approach), revealing that a better class separability is achieved. As for the *crack* regions intraclass to interclass distances ratio, a better value is again achieved for the first approach showing a better clustering of crack regions points (ratios of 0.217 and 0.246 for the first and second approaches, respectively). The *no crack* ratios are better than those of unprocessed images (0.366). This same tendency can be observed for *crack regions* ratios (0.374), showing that region intensity normalization and saturation procedures leads to improvements over the original feature space, with the two classes becoming more separable.

Table II lists precision, recall and performance criterion (PC) metrics [7] for the detection of regions with crack pixels.

According to the values of Table II, the second sequence of

procedures produces better PC values, but since for this type of application the detection of regions with cracks is more important, the first approach leads to better results. Notably, recall (96.75% vs. 93.96%) is more important than precision for this type of application. Both pre-processing orderings produce better results than the usage of unprocessed images, showing their utmost relevance in terms of detecting regions with crack pixels.

Table II  
Evaluation metrics

Procedures	Recall (%)	Precision (%)	PC (%)
Norm + Saturation	96.75	87.30	91.45
Saturation + Norm	93.96	90.70	91.95
Original	82.25	91.90	86.12

### IV. CONCLUSIONS AND FUTURE WOK

This paper discusses the components of the pre-processing module of a road crack detection system, and the different ways to combine them. The proposal consisting of region intensity normalization followed by intensity saturation enhance the detection of regions with crack pixels, showing good recall values, without losing significantly on the overall system performance due to a better class separability.

Future developments may consider a reject-option and the usage of a non uniform loss function, since false positive detections often have less impact on this type of application. Also, the search for other features with better interclass and intraclass distance properties, eventually using texture analysis will be addressed.

### REFERENCES

- [1] H. Zhang, Q. Wang, "Use of Artificial System for Pavement Distress Survey", in *Proc. 30th Conference of the IEEE Industrial Electronics Society*, Busan, Korea, 2-6 November, 2004, pp. 2486-2490 Vol.3.
- [2] H.D. Cheng, M. Miyojim, "Automatic Pavement Distress Detection System", *Journal of Information Sciences 108*, pp. 219-240, ELSEVIER, July 1998.
- [3] H. Oliveira, P.L. Correia, "Supervised Strategies for Crack Detection in Images of Road Pavement Flexible Surfaces", in *Proc. 16th European Signal Processing Conference (EUSIPCO 2008)*, Lausanne, Switzerland, 25-29 August, 2008.
- [4] M. Figueiredo: "Lecture Notes on Bayesian Estimation and Classification", <http://www.lx.it.pt/~mtf/learning/>, Portugal, 2004.
- [5] R. Duin, P. Juszczak, P. Paclik, E. Pekalska, D. Ridder, D. Tax: "PRTools 4 - A MatLab Toolbox for Pattern Recognition - version 4.0.23", <http://www.prtools.org/>, Netherlands, 2004.
- [6] F. Heijden, R. Duin, D. Ridder and D. Tax, "Classification, Parameter Estimation and State Estimation - an engineering approach using MatLab", John Wiley & Sons, 2004.
- [7] D. Tax: "Data Description Toolbox", [http://ict.ewi.tu.delft.nl/~davidt/dd\\_tools.html](http://ict.ewi.tu.delft.nl/~davidt/dd_tools.html), Netherlands, 2006.